Electron Technology, 2, 2/3, pp. 149–158. Institute of Electron Technology P.A. Sci., Warsaw 1969

LASER ENERGY, POWER AND FREQUENCY MEASUREMENTS[1]

Pomiary energii, mocy i częstotliwości laserów

Les mesures de l'énergie, de la puissance et de la fréquence des lasers

Измерения энергии, мощности и частоты лазеров

DONALD A. JENNINGS, KENNETH M. EVENSON, WILLIAM R. SIMMONS, AND ALVIN L. RASMUSSEN
National Bureau of Standards, Boulder, Colorado

INTRODUCTION

THE PURPOSE of this paper is to discuss briefly some of the work being done at the National Bureau of Standards with regard to laser standards. The areas involved are: pulsed laser energy measurement, CW laser power measurement and HCN laser frequency measurement. We will discuss the method used, how the method may be used to calibrate other power and energy measuring devices, and the accuracy of the particular method. Frequency measurements of the HCN laser are discussed because of their relevance to frequency stabilized lasers.

PULSED LASER ENERGY MEASUREMENTS

Of the several methods one may use to measure pulsed laser energy [1–8], the calorimetric method is capable of yielding relatively high accuracy. We have designed, built and, calibrated calorimeters for measuring the output energy of the pulsed ruby laser, 694.3 nm. A system has been devised for intercomparing these calorimeters with other energy measuring devices over an energy range from 1 to 100 J with an estimated accuracy of ± 2.0 percent. This specific calorimeter has been designed to measure energies to 10 J/cm^2 and peak powers to 200 MW/cm^2.

Many of the details are given in Ref. 8 by Donald A. JENNINGS. They are reviewed partially here and modified according to the additional work accomplished.

The calorimeter is shown in Fig. 1. The calorimeter absorption cell, filled with an energy absorbing solution, is supported in an aluminum heat sink by polystyrene foam. The aluminum heat sink is also placed in polystyrene foam insulation and the entire system enclosed in an aluminum box. One junction of a Cu-Constantan thermocouple is attached

(1) Contribution of the National Bureau of Standards, Not Subject to Copyright.

with silver epoxy to the absorption cell, and the other junction is attached to the aluminum heat sink. When a pulsed laser is fired into the absorption cell, the cell rises in temperature and the thermocouple generates a voltage proportional to the temperature difference between the absorption cell and the aluminum heat sink. The decaying output voltage

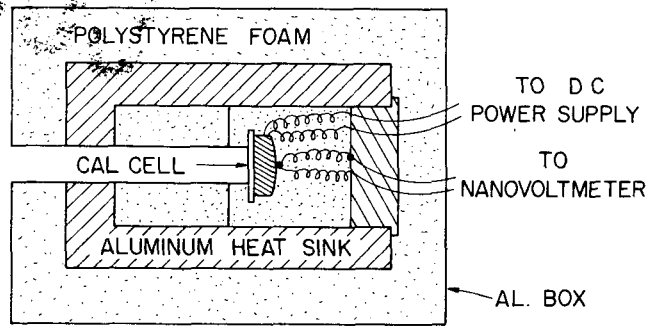

FIG. 1. Cross-sectional diagram of the calorimeter, showing layout of components, method of insulating and supporting the calorimeter absorption cell, and position of the thermocouple.

of the thermocouple, logarithmically extrapolated to time zero, is a measure of the energy in the laser beam. The voltage generated by the thermocouple is measured with a nanovoltmeter whose output is amplified and fed into a strip chart recorder.

A cross-sectional view of the absorption cell is shown in Fig. 2. The cell wall is made of silver $\sim$ 0.5 mm thick. The cell has a diameter $\sim$ 3 cm and a depth of 3 mm at the

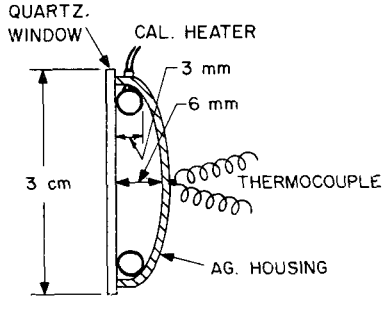

FIG. 2. Cross-sectional diagram of the calorimeter absorption cell, showing the approximate size of components and the position of the heater wire.

edge and 6 mm at the center. It has two small holes near the edge. One hole is utilized for filling liquid and the other one is for the heater wires. The heater wire has a teflon coating a resistivity of 16 ohms/foot and a total resistance $\sim$ 100 ohms. The entrance window is a high optical quality quartz. A cement, used to bond materials with dissimilar expansivities, glues the quartz window to the silver cell. A small amount of beeswax and epoxy is used to seal the fill and heater wire holes. The cell is filled with a one molal solution of $CuSO_4 \cdot 5H_2O$. The addition of a few drops of Bendix purple ink into the solution extends the useful range to < 500.0 nm. The absorption characteristic of the solution is nearly the same at 694.3 nm and 1060.0 nm, although there is a large increase in it between these

two wavelengths. The cell filled with this solution will absorb > 99.9 percent of the laser beam, not including the Fresnel reflection at the entrance window which is 3.5%.

The cell gives about 0.1°C temperature rise for a $\frac{3}{4}$ J input.

Two independent methods of calorimeter calibration are used. One calibration is based on the heat capacity of the absorption cell and the thermocouple calibration; and the second, on a *dc* electrical energy substitution using the heater wire. A correction is made for Fresnel reflection at the entrance window.

The heat capacity calibration consists of weighing all the component parts of the absorption cell and using the most accurate obtainable values for the specific heats to calculate the heat capacity of the absorption cell.

The thermocouple sensitivity is calibrated using standard techniques. The thermocouple is attached to the cell using a high thermoconductivity silver epoxy. The thermocouple must have close thermocontanct with the cell to yield correct temperature changes between the cell and the heat sink.

The *dc* electrical energy substitution calibration is accomplished by passing a known *dc* current through the heater wire for a known length of time. The calibrated value is obtained by making a logarithmical extrapolation of the thermal decay to time zero. The calibration values are given in μV/J input. The two calibrations agree within 1%.

To intercompare calorimeters and other detectors, we use the apparatus arrangement shown in Fig. 3, 4, and 5. We evaluate the energies received E and the reflectivities R.

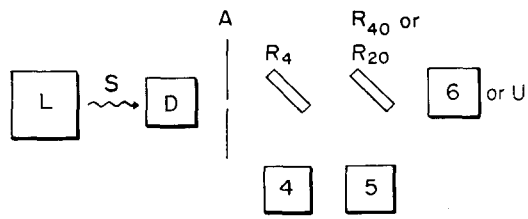

FIG. 3. Block diagram of apparatus arrangement used to intercompare pulsed laser energy measuring devices. Laser L, demagnifier D, aperture A, NBS calorimeters *4, 5, 6* and device U, and beam splitters R_4, R_{20} and R_{40} with reflectivities 4, 20, and 40% respectively. D reduces the diameter of laser beam to $\sim$ 1/4 size. A = 3/8″, etc. depending on devices to be calibrated.

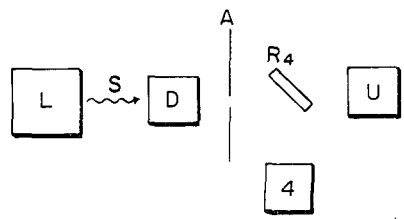

FIG. 4. Same as Fig. 3 with the second beam splitter removed.

These are approximately 4%, 20%, and 40% for R_4, R_{20} and, R_{40}, respectively. R_4 can be used for making measurements from $\sim$ 20 to 100 J; R_{20}, 5 to 20 J; and R_{40}, 1 to 5 J. R_4 and R_{20} are used together because of the maximum energy limits of the NBS calorimeters.

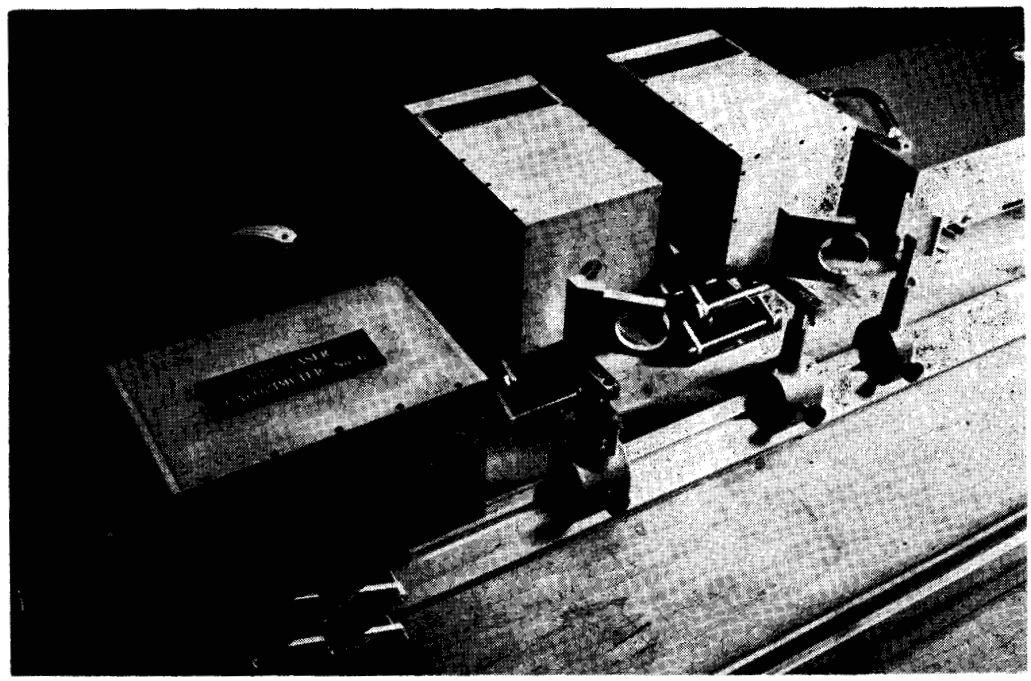

FIG. 5. Photograph of apparatus arrangement of Fig. 3 with laser L and demagnifier D not showing.

The energy input to the unknown device, E_u, is evaluated after determining the energies and the reflectivities of the components in Fig. 3 and Fig. 4.

We have

$$R_{20} = \frac{E_5}{E_5 + E_6}$$ See Fig. 3. Laser output S. Calorimetr 6 used.

$$R_4 = \frac{E_4'}{\frac{E_5'}{R_{20}} + E_4'}$$ See Fig. Laser output S'. Device U used.

And finally

$$E_u'' = \left(\frac{1-R_4}{R_4}\right) E_4'' = \frac{E_5'}{\left(\frac{E_5}{E_5+E_6}\right) E_4} E_4''$$ See Fig. 4. Laser output S''.

Since $E_6 \approx 4E_5$, the accuracy of E_u'' depends mostly upon the accuracy of E_6.

When R_{20} and R_{40} are used to determine the energy E_u, we have

$$E_u' = \left(\frac{1-R_{20}}{R_{20}}\right) E_5',$$

when R_{20} is used,

or

$$E_u' = \left(\frac{1-R_{40}}{R_{40}}\right) E_5',$$

when R_{40} is used.
And

$$E_u' = \frac{E_6}{E_5} E_5',$$

where

$$\frac{E_6}{E_5} \quad \text{for } R_{20} \quad \neq \frac{E_6}{E_5} \quad \text{for } R_{40}.$$

Again the accuracy of E_u' depends upon the accuracy of E_6.

Using R_4 and R_{20} to calibrate a calorimeter, gives values which are within one percent of each other. Using R_{20} and R_{40} to calibrate another calorimeter gives similar agreement. The beam splitters need to be recalibrated from time to time because the laser alinement may change slightly. The NBS calorimeters need to be recalibrated occasionally to check the absorption cells for leakage.

The sum of the calibration uncertainties of the NBS calorimeters and the system is $\pm 2\%$.

CW Powers Measurements

The need often arises while working with CW lasers for measuring the absolute power in the laser beams. There are many portable power meters that will make this measurement, but their calibration is usually in doubt. The calorimeter used for pulsed laser energy measurements as described earlier lends itself to the task of absolute power calibration of power meters. Since the calorimeter and its associated equipment have already been calibrated, it can be used as a device to integrate the power of a CW laser beam for a measured period of time from which the average power can be determined. However, due to the necessity of using long integration times, on the order of 1 to 2 minutes, the heat losses from the calorimeter cell during the initial temperature rise are not the same as for the pulse laser energy measurement. It is necessary therefore to use an electrical calibration pulse of the same power level and same time duration as the CW laser pulse.

A schematic representation of the CW laser power meter calibration unit used in this laboratory is shown in Fig. 6. The function of each component is as follows: the timer--shutter control actuates the shutter and precisely controls the time during which the laser beam enters the unit. In addition it provides a time reference for the two chart recorders. The beam splitter, B, divides the beam into two parts; one parts is directed towards the transfer detector and the other part illuminates the calorimeter cell, C. A diffusing screen is placed before the silicon photovoltaic cell in the transfer detector to provide more even illumination and to prevent damage of the photocell surface. Two recorders record the output of the transfer detector and the calorimeter as a function of time. The time reference is recorded on the second channel in each. R, which terminates the output of the transfer detector, is chosen such that the maximum illumination of the transfer detector will not produce a nonlinear output of the photocell. The achromatic lens, L_2, provedes a divergent beam to accomodate power meter sensing heads with different diameter apertures. Lens L_1 produces an image, I, on the alignment screen of the beam spot on the transfer detector.

This provides a convenient means of checking the alignment of the calibration unit with respect to the incoming laser beam throughout the entire calibration.

The calibration procedure consists of two parts. In the first part the output of the transfer detector is calibrated in terms of absolute power in the laser beam as seen by the

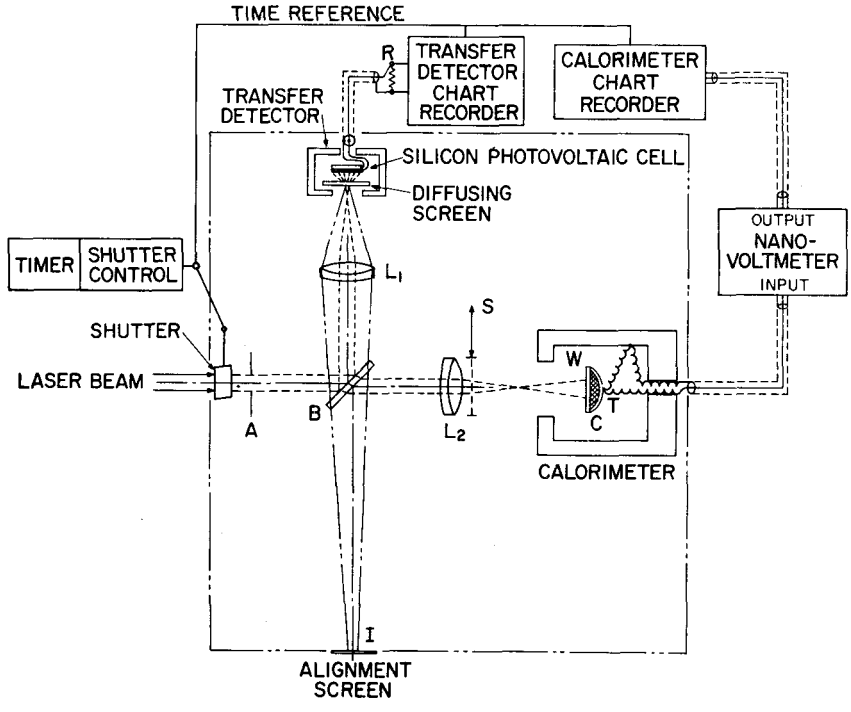

FIG. 6. CW laser power meter calibration unit.

calorimeter. Schematically this is shown in Fig. 7. After the calibration unit has been aligned with the laser beam, the timer is set for a time τ and the shutter is activated. The output of the transfer detector in millivolts is recorded on one chart recorder as a function of time. Simultaneously the output of the calorimeter is recorded on the other recorder as a function of time. The reference time pulse on the transfer detector recorder provides a check of zero time and on the other it determines zero time.

The output of the calorimeter begins to rise with the onset of the laser beam and the light energy is converted to heat energy. It continues to rise after the shutter is closed until an equilibrium is reached after which cooling takes over and the output decreases. Previously it has been shown that the cooling is predominantly that due to Newton's law of cooling and hence fits an exponential decrease. Thus by using data points to fit an exponential and knowing the calibration constant (determined as described earlier) in microvolts per joule of the calorimeter, the total electromagnetic energy incident on the calorimeter for the time, τ, can be determined.

The average power then leaving lens L_2 is known for one power level input. Repeating this procedure for other power levels into the calibration unit yields a straight line graph

of millivolts output of the transfer detector as a function of the laser beam power leaving lens L_2 for one wavelength.

The second and last part of the calibration is performed by replacing the calorimeter with the sensing head of the power meter to be calibrated. Since the output transfer detector is now calibrated in terms of the power incident on the power meter sensing head, it is merely necessary to compare outputs and the calibration is complete.

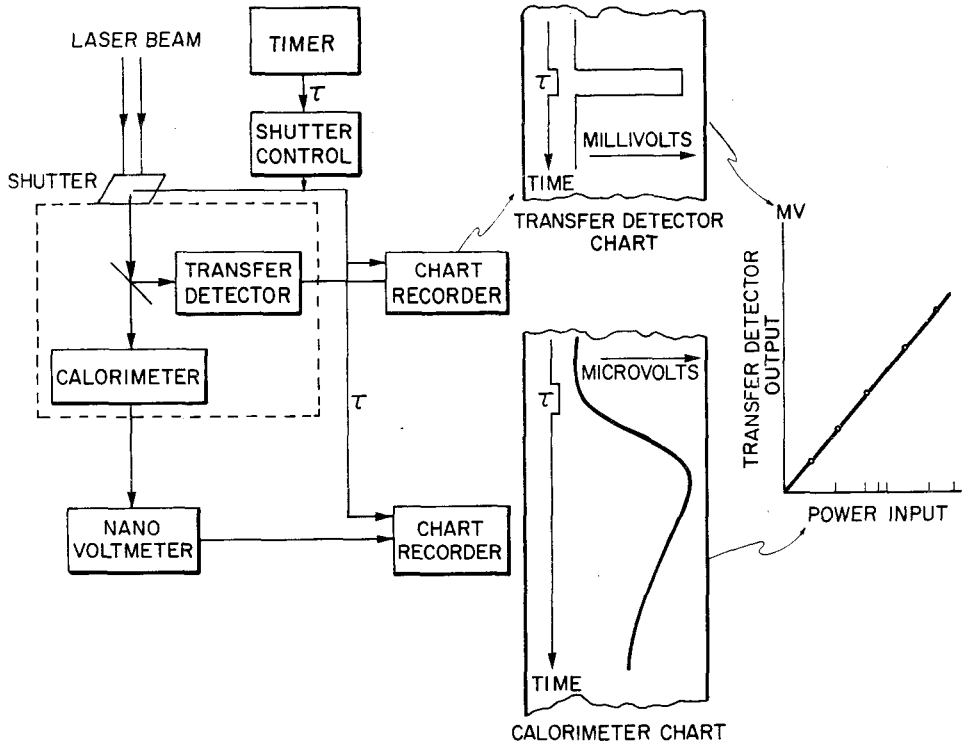

FIG. 7. Transfer detector calibration.

Figures 8 and 9 show data obtained during a power meter calibration. The three wavelengths used were 514.5 nm and 488.0 nm lines from an argon ion laser and the 632.8 nm line from a helium neon laser. Various power levels in the beam were obtained by varying the input power to the laser.

One of the calorimeter output recordings is shown in Fig. 8. The illumination was the 488.0 nm line. The two points shown are examples of the points used to determine the constants of the exponential cooling curve; the equation of which is also shown. The average power seen by the calorimeter in this case was 11.7 milliwatts as determined by projecting the cooling curve to $t = 0$. Also indicated by the event marker is the time, 104 seconds, that the laser beam illuminated the calorimeter. It may also be seen that a straight line projected back to zero time (dashed line) yields a value of average power close to the value obtained from the exponential.

The results of the first part of the calibration procedure, namely calibration of the transfer detector are shown in Fig. 9. The values of the ordinates for the plotted points shown were obtained from curves like Fig. 8. Values for these data point abscissae were obtained from the output of the transfer detector as measured across a five ohm termina-

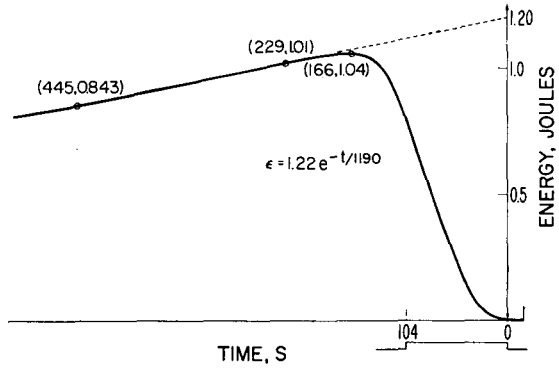

FIG. 8. Calorimeter response curve.

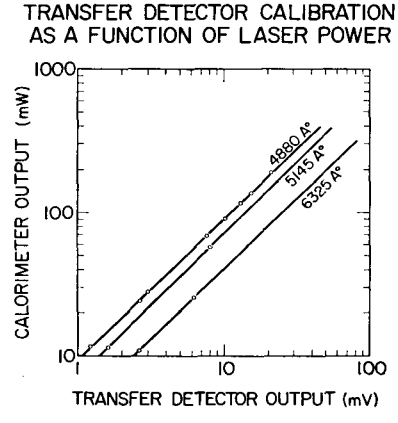

FIG. 9. Transfer detector calibration as a function of laser power.

ting resistor with a calibrated chart recorder. The chart recorder also provided a monitor of the laser beam during the time of illumination. Since the curve for the 488.0 nm line was linear, it was assumed the curves for 514.5 and 632.8 nm lines would also be linear and only two data points were used.

The last part of the calibration was completed by replacing the calorimeter with the sensing head of the power meter and comparing the power meter readings with the curves of Fig. 9.

The worst-case estimated error in a single point on the curves of Fig. 9 is approximately $\pm 6\%$. This value was determined from the following data: an estimated error of 1% is associated with the calorimeter-nanovoltmeterchart recorder calibration. In fitting the exponential curve of Fig. 8, it is estimated that the coefficient of the exponential which is the energy into the calorimeter is determined to within $+1.3\%$. The timer used here has

an uncertainty for the shortest time of $\pm 0.8\%$ plus a $\pm 1\%$ uncertainty in the shutter activation. The maximum deviation in the laser beam from a constant value during illumination is 2%. A measure of the precision is indicated in Fig. 8 by how well the data points fit the straight line.

FREQUENCY MEASUREMENTS IN THE FAR-INFRA-RED

The frequencies of the 337 and 311 μm HCN laser lines as measured by NBS are 890,759.4±0.1 and 964,312.1±0.2 MHz, in agreement with similar measurements by HOCKER et al [9]. Our early frequency measurements were made by observing the beat note between the 12th and 13th harmonics of a phase locked 74 GHz klystron and the two HCN laser lines in a crossguide harmonic generator-detector with 1.88 × 3.73 mm and

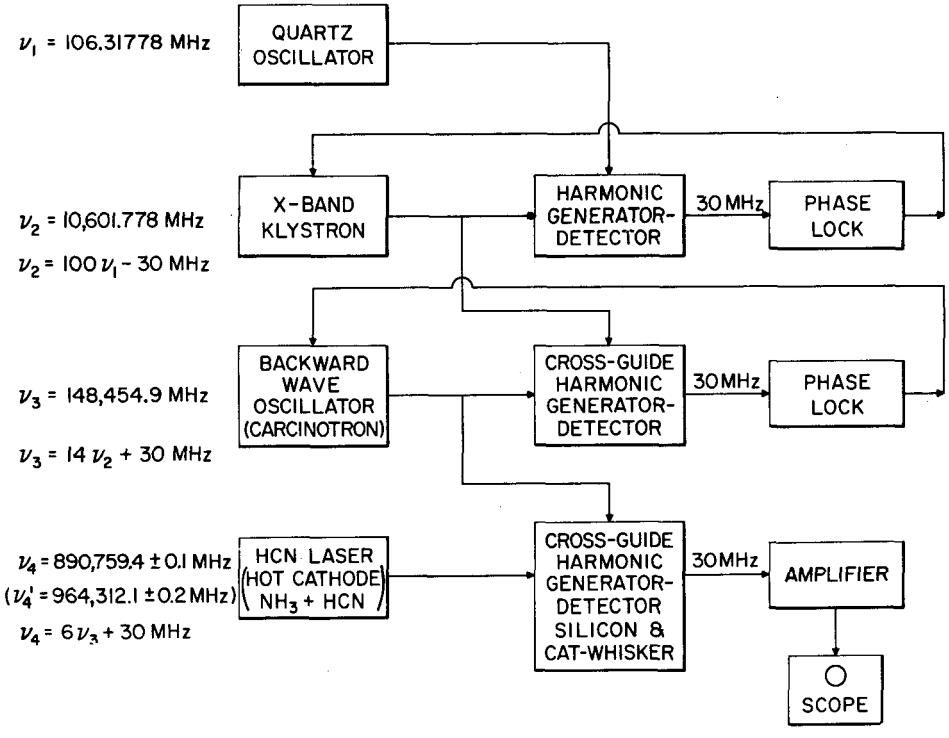

FIG. 10. HCN laser frequency measurement block diagram.

0.65 × 1.30 mm waveguides. A tremendous increase in the signal to noise of the beat note was found by beating the laser with the 6th harmonic of a 148 GHz carcinotron as shown in Fig. 10. The beat note was about 2 KHz wide when displayed on a spectrum analyser. To obtain this narrow beat note, high spectral purity of ν_1 is provided by an exact frequency crystal oscillator, and a very stable laser output.

Four invar rods were used as mirror spacers to provide both thermal and mechanical stability. An extremely stable electrical discharge was achieved using a regulated voltage dower supply, a hot cathode, and a mixture of HCN and NH_3 in the laser. The imodıpev

signal-to-noise of the beat note should allow phase or frequency locking of the laser. If these attempts are successful, similar experiments will then be tried with the 118 μm water vapor laser. The plan is the eventual use of these frequency sources as steps toward frequency measurements in the optical region. The possibility of simultaneous frequency and wavelength measurements yielding the speed of light is also being considered.

REFERENCES

1. G. BIRNBAUM and M. BIRNBAUM, Proc. IEEE, **55**, 6, 1026, 1967.
2. D. E. KILLICK, D. A. BATEMEN, D. R. BROWN, T. S. MOSS and E. T. DE LA PERRELLE, Infrared Phys., **6**, 85, 1966.
3. A. J. SCHMIDT and R. C. GREENHOW, J. Sci. Instr., **44**, 468, 1967.
4. J. G. EDWARDS, J. Sci. Instr., **44**, 835, 1967.
5. H. S. HEARD, *Laser Parameter Handbook*, (John Wiley D Sons, New York, 1968), pp. 480.
6. R. A. VALITOV, YU. A. KALININ and V. M. KUZ'MICHEV, Translated from Izmeritel'naya Tekhnika, no. 5, 37, May 1965.
7. A. V. KUBAREV, A. S. OBUKHOV, A. YA. LEIKIN, Y. S. SOLOV'EV and V. P. KORONKEVICH, Translated from Izmeritel'naya Tekhnika, no. 11, 20 Nov. 1967.
8. D. A. JENNINGS, IEEE Trans. on Instr. D Meas. IM-15, no. 4, 161, Dec. 1966.
9. L. O. HOCKER, A. JAVAN, D. R. RAO, L. FRENKEL, and T. SULLIVAN, Appl. Phys. Letters, **10**, 147, 1967.

DISCUSSION

L. FRENKEL: By turning your calorimeter vertical, could you not eliminate all windows?

Answer: This is true, but a very serious thing then happens the calibration keeps changing because of evaporation of the liquid.

K. KANTOR: Don't you have disturbing interference at the quartz window?

Answer: No, since we only have one air glass interface giving about 3.5% reflection, the other is a liquid glass interface ($n = 1.48$, $n_g = 1.33$) gives about 0.2% reflection. This turns out to be very small considering the other errors we have.

L. ESSEN: I should like to ask whether the figure of 1×10^{-7} is a difference from other measurements or the accuracy of the measurement?

Answer: I think the figure of 1×10^{-7} represents our accuracy at the time of. However we have been able to do about a part 3×10^{-9} and as I recall there is no difference.